JOURNAL OF MATERIALS SCIENCE 17 (1982) 17–30

# Constitution, structure and magnetic properties of some rare-earth–cobalt–aluminium alloys

J. EVANS, I. R. HARRIS
*Department of Physical Metallurgy and Science of Materials, University of Birmingham, Birmingham, UK*

The constitution and structure of the alloys represented by the formulae $Ce_{1-x}Al_xCo_5$ and $Pr_{1-x}Al_xCo_5$ (where $0 \leqslant x \leqslant 0.6$) have been studied by X-ray diffraction and metallographic techniques. The substitution of between 1 and 3 at % Al ($0.06 \leqslant x \leqslant 0.18$) for Ce in $CeCo_5$ produces a mixture of the 1:5 and 2:17 phases based on $CeCo_5$ and $Ce_2Co_{17}$; there are two variations of the 2:17 phase which are isostructural with the hexagonal $Th_2Ni_{17}$-type and rhombohedral $Th_2Zn_{17}$-type phases. At the composition $Ce_{0.76}Al_{0.24}Co_5$ (4 at % Al) the alloy consists only of the 2:17-type phases and metallographically the alloy is one phase in appearance. Further substitution of Al results in the precipitation of an fcc phase, based on the Co–Al solid solution, in the 2:17 matrix. The crystal structures of the $Pr_{1-x}Al_xCo_5$ alloys are very similar to those of the equivalent cerium alloys, although the ternary 2:17-type phase has only the rhombohedral structure, as does the binary $Pr_2Co_{17}$ phase. The metallographic structures of the Pr alloys in the composition range 1 to 3 at % Al show significant differences from the corresponding Ce alloys. Determination of the Curie temperatures of the $R_{1-x}Al_xCo_5$ alloys ($R$ = Ce and Pr) in the composition range $0 \leqslant x \leqslant 0.24$ showed good agreement between the measured and published values for both the $CeCo_5$ and $PrCo_5$ phases. The Curie temperatures of the ternary 2:17-type phases were approximately 50 K and 70 K lower than those of the binary, $Ce_2Co_{17}$ and $Pr_2Co_{17}$ alloys, respectively.

## 1. Introduction

The excellent permanent magnetic properties of the $RCo_5$ compounds (notably $SmCo_5$) result from their magnetic anisotropy which is related to their crystal structure [1, 2]. The permanent magnetic characteristics are governed by domain considerations and Washko *et al.* [3] have suggested that ternary 1:5 compounds of Sm and Co with a non-transition, non-rare-earth element might yield good magnetic properties since the third alloying constituent might widen the solubility limits of the 1:5-type phase, and introduce domain wall pinning sites for raising the intrinsic coercive force. These authors found that as Hf and Mg were partially substituted for Sm in $SmCo_5$, to form phases represented by the general formulae $Sm_{1-x}Hf_xCo_5$ and $Sm_{1-x}Mg_xCo_5$, the intrinsic coercivity and remanence while decreasing with Hf and Mg content still remain remarkably good; Hf substitutions stabilize the 1:5 structure while Mg substitutions favour the 2:17 structure.

The presence of any $Sm_2Co_{17}$ in unsubstituted $SmCo_5$ lowers the intrinsic coercivity because the 2:17 phase provides regions for the production of reverse domains. However, a new generation of rare-earth–transition-metal magnetic alloys have been produced that are based on the 2:17 structures. These alloys have rather complicated formulae (consisting of five or more elements) and depend for their good magnetic properties on the high remanence of the 2:17-type phases and a very finely distributed precipitate (possibly of a 1:5-type phase) which provides domain pinning sites and greatly increases the rather low intrinsic

0022–2461/82/010017–14$03.40/0  

coercivities of the binary 2:17 phases. Comprehensive reviews of the 1:5- and 2:17-type magnetic materials are given in [4, 5].

In the present work the alloy systems $R_{1-x}Al_xCo_5$ ($R$ = Ce and Pr) have been investigated and these alloys have been found to be one-phase or two-phase in character, depending on their composition, and to exhibit both the 1:5- and 2:17-type structures. Thus a study of these systems should provide information on phase stability and on the influence of structure on the magnetic properties.

## 2. Materials and experimental methods

The cerium and praseodymium used in the present investigation were obtained from Rare Earth Products Ltd, the metals were prepared from 99.9% grade oxide which, according to the manufacturers, contained not more than 200 ppm of base metals. The aluminium and cobalt were obtained from Koch Light Laboratories Ltd, and were of nominal purities 99.999% and 99.998%, respectively.

The alloys were prepared by arc melting in an argon atmosphere. In general, weight losses on melting were small and for all the cerium alloys and for the praseodymium alloys up to and including $Pr_{0.76}Al_{0.24}Co_5$ ($x \leqslant 0.24$), composition of the alloys can be taken to be within ± 0.4% of the nominal compositions. For the Pr alloys containing more than 4 at% Al ($x > 0.24$) there was very little weight loss on melting but the praseodymium seemed to form a "skin" on the surface of the alloys which flaked off on exposure to air. After repeated melting and prolonged annealing it was possible to obtain samples in the composition range $Pr_{0.70}Al_{0.30}Co_5$ to $Pr_{0.40}Al_{0.60}Co_5$ that appeared homogeneous and did not deteriorate on exposure to air, but the weight losses in these alloys were greater than those in the other samples. All the alloys were homogenized for 10 days at a temperature of 1250 K.

After homogenization, the specimens were cut in two in a direction perpendicular to the plane of the copper hearth on which they were melted; this was done to show the directional effect of cooling from the melt on the structure of the alloys. After being cut, the alloys were ground, diamond polished and etched in nital. The etched specimens were photographed using a Zeiss Ultraphot microscope.

The powders for X-ray analysis were annealed for 2 h at 1223 K and then exposed to CoKα radiation in a Philips Debye–Scherrer camera (of 11.483 cm diameter). The lattice spacings were derived from the diffraction patterns using the Nelson–Riley extrapolation function and an iterative method was used to obtain refined values of the axial ratio, $c/a$, and of the $a$-spacing. The relative intensities of the X-ray lines were measured using a double-beam Joyce microdensitometer. A trace of the lines on the Debye–Scherrer films was recorded and the area of a particular diffraction peak was measured using a planimeter. The reproducibility of each measurement varied from approximately ± 5% for strong lines to approximately ± 10% for weak lines.

The Curie temperatures of the samples were measured using a modified Faraday method. A Sartorius vacuum electro–microbalance was used in conjunction with a Newport electromagnet which gave a maximum flux density between the poles of 0.4 Tesla, and a non-inductively wound furnace was employed in heating the samples to a temperature of about 1223 K.

## 3. Experimental results and discussion

### 3.1. X-ray results

#### 3.1.1. The $Ce_{1-x}Al_xCo_5$ system

$CeCo_5$ has the hcp, $CaZn_5$-type structure. On the addition of Al to $CeCo_5$, two new phases appear; these are isostructural with the two forms of the $Ce_2Co_{17}$ structure, the hexagonal $Th_2Ni_{17}$-type (space group $P6_3/mmc$) and the rhombohedral $Th_2Zn_{17}$-type (space group $R\bar{3}m$) [6]. In the present work the structures of both the 2:17 phases are indexed as pseudo-hexagonals.

The diffraction patterns of the alloys $Ce_{0.94}Al_{0.06}Co_5$, $Ce_{0.88}Al_{0.12}Co_5$ and $Ce_{0.82}Al_{0.18}Co_5$ indicate that they are all three-phase, consisting of the original $CeCo_5$ and the two modifications of the $Ce_2Co_{17}$-based structure.

The lattice parameters of the $CeCo_5$-phase present in the binary and ternary alloys are listed in Table I. It is seen that, within the experimental error of ± 0.0005 Å, there is virtually no variation

TABLE I Lattice parameters of the $CeCo_5$ phase in the $Ce_{1-x}Al_xCo_5$ alloys

| Sample Composition | | $a$ ($c/a$ = 0.815) (Å ± 0.005) |
|---|---|---|
| $x$ | at% Al | |
| 0 | 0 | 4.9292 |
| 0.06 | 1 | 4.9287 |
| 0.12 | 2 | 4.9292 |
| 0.18 | 3 | 4.9300 |

TABLE II Lattice parameters of the $Ce_2Co_{17}$-type phases in the $Ce_{1-x}Al_xCo_5$ alloys

| Sample Composition | | $Th_2Zn_{17}$-type structure $a$ (Å ± 0.002) ($c/a$ = 1.458) | $Th_2Ni_{17}$-type structure $a$ (Å ± 0.002) ($c/a$ = 0.972) |
|---|---|---|---|
| $x$ | at % Al | | |
| 0.06 | 1 | 8.367 | 8.368 |
| 0.12 | 2 | 8.365 | 8.365 |
| 0.18 | 3 | 8.368 | 8.368 |
| 0.24 | 4 | 8.367 | 8.367 |
| 0.30 | 5 | 8.380 | 8.382 |
| 0.36 | 6 | 8.391 | 8.390 |
| 0.42 | 7 | 8.394 | 8.399 |
| 0.48 | 8 | 8.404 | 8.406 |
| 0.54 | 9 | 8.402 | 8.405 |
| 0.60 | 10 | 8.412 | 8.412 |

in lattice parameter with increasing Al-content for this phase, i.e. there is no significant substitution of Ce by Al in the $CeCo_5$-phase.

The lattice parameters of the two 2:17 phases were also obtained using the refinement method, though only one high angle line could be positively identified for each phase. The $c/a$ ratios of the two phases were identical with those found by Ostertag and Strnat for $Ce_2Co_{17}$ [6] though the $d$-spacings, and hence the $a$ and $c$ parameters, were larger. The $a$-spacings are listed in Table II and plotted as a function of sample composition in Fig. 1. It is seen that, within the experimental error of ± 0.002 Å, the values for the rhombohedral and hexagonal phases are identical. In the composition range between 1 and 4 at % Al the spacing is constant. Between 5 and 8 at % Al, there is an almost linear increase in parameter with increasing Al content and beyond this point the change in the $a$-spacing with composition levels off. An extrapolation from the composition range where there is a linear variation of $a$ with % Al, to the 0 % Al composition gives a value that is similar to, but slightly higher than, the value quoted in [6] for the $\alpha$-parameter of the binary $Ce_2Co_{17}$ phases.

The diffraction patterns of the alloys $Ce_{0.76}Al_{0.24}Co_5$ and $Ce_{0.70}Al_{0.30}Co_5$ only exhibited lines from the 2:17 phases though it was shown metallographically (Fig. 3) that the latter sample contained a small amount of two-phase material.

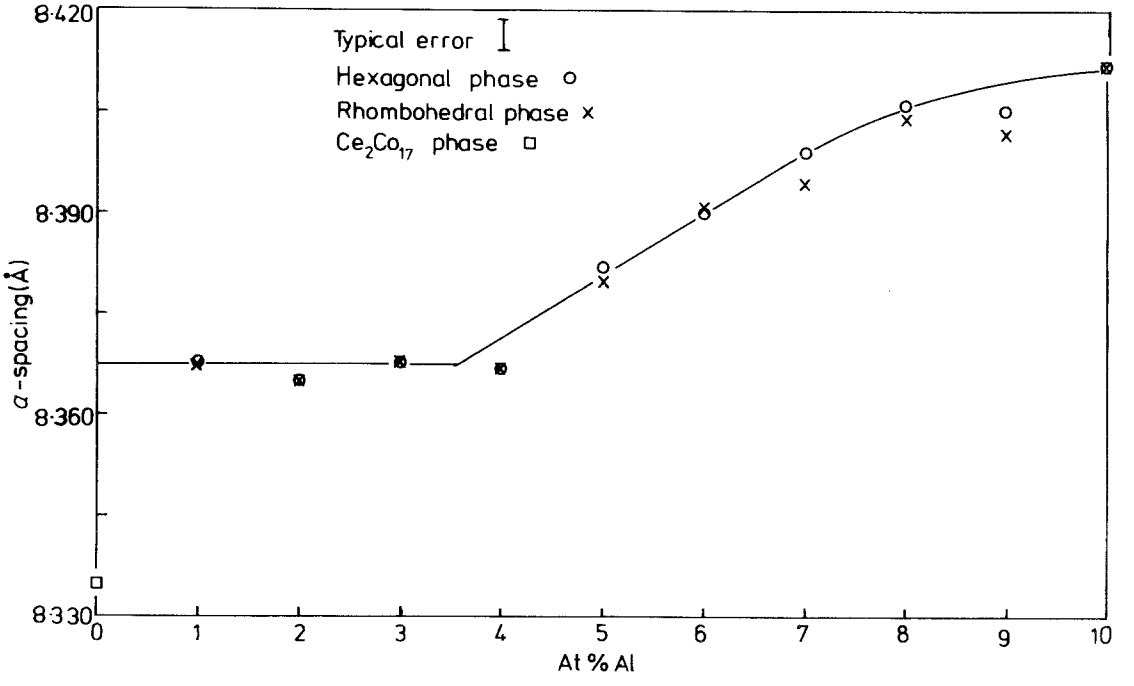


*Figure 1* Lattice spacings of the $Ce_2Co_{17}$-type phases against composition of the Ce–Co–Al alloys.

TABLE III Lattice parameters and compositions of the Co–Al phase in the $Ce_{1-x}Al_xCo_5$ alloys

| Sample composition | | $a$-spacing (Å ± 0.001) | Percentage of Al in the βCo–Al phase (± 0.5%) |
|---|---|---|---|
| $x$ | at% Al | | |
| 0.36 | 6 | 3.544 | 4.5 |
| 0.42 | 7 | 3.556 | 5.4 |
| 0.48 | 8 | 3.562 | 8.3 |
| 0.54 | 9 | 3.563 | 9 |
| 0.60 | 10 | 3.563 | 9 |

The $Ce_{0.76}Al_{0.24}Co_5$ sample appeared to be one-phase (Fig. 3), and it was not possible to differentiate metallographically between the two modifications of the $Ce_2Co_{17}$ structure. The diffraction patterns of the other five alloys in the series (containing from 6 to 10 at% Al) showed reflections from the two 2:17 phases and from a fcc phase which was identified as a solid solution of Al in the high temperature phase of cobalt (βCo).

The intensities of the reflections from the βCo–Al phase increase regularly with increasing percentage of Al in the alloys, as does the lattice parameter of the fcc phase. Luo and Duwez [7] have determined the lattice parameter variation of the βCo–Al solid solutions with Al and their results have been used to calculate the compositions of this phase in the $Ce_{1-x}Al_xCo_5$ alloys, assuming that there is no solubility of cerium in the fcc phase. This assumption is consistent with the published Ce–Co phase diagram [8] which indicates negligible solubility of Ce in βCo. The results are listed in Table III.

From the micrographs of the alloys containing from 6 to 10 at% Al, the relative amounts of the βCo–Al solid solution and the 2:17 phases were determined and, using the results listed in Table III, the compositions of the 2:17 phases in these alloys have been derived. The results are listed in Table IV, the amount of each constituent being determined to an accuracy of approximately ± 1 at%. From these results it has been shown that the amount of Al in the 2:17 phase increases linearly with the Al concentration of the alloy [9], the amount of Co falls slightly and the Ce content varies somewhat erratically, though this variation is not really signficant compared to the experimental error. The total amount of non-rare-earth constituent (Co + Al) also remains virtually constant, though at a level below that of stoichiometric $Ce_2Co_{17}$ (10.53 at% Ce, 89.47 at% Co).

Although both modifications of the 2:17 structure were present in all the alloys in the composition range 4 to 10 at% Al, the relative intensities of the reflections from the rhombohedral phase [9] seem to be greater (compared to those from the hexagonal phase) than those quoted by Ostertag and Strnat [6]. As these authors associated the rhombohedral phase with the rare-earth-rich side of the 2:17 homogeneity region, it seems as though the ternary 2:17 phases present in the $Ce_{1-x}Al_xCo_5$ alloys are rare-earth-rich and behave in a similar way to the binary $Ce_2Co_{17}$ compound. This is consistent with the Ce concentrations given in Table IV.

### 3.1.2. The $Pr_{1-x}Al_xCo_5$ system

$PrCo_5$, like $CeCo_5$, has the $CaZn_5$ structure and the alloys, $Pr_{0.94}Al_{0.06}Co_5$, $Pr_{0.88}Al_{0.12}Co_5$ and $Pr_{0.82}Al_{0.18}Co_5$ are all two-phase, consisting of the original $PrCo_5$-phase and a rhombohedral, $Th_2Ni_{17}$-type structure, isotypal with $Pr_2Co_{17}$. The lattice parameters of the $PrCo_5$ phase are listed in Table V and, within the experimental error of ± 0.001 Å, there is no significant variation in lattice parameter with increasing Al-content for this phase. This indicates that there is no significant substitution of Pr by Al in this phase.

The $c/a$ ratio of the 2:17 phase is identical with that found by Ostertag and Strnat [6] for $Pr_2Co_{17}$ (1.446) but smaller than that found by Buschow [10] (1.455). The $a$-spacings are listed in Table VI and plotted in Fig. 2; it can be seen that, in the composition range 1 to 4 at% Al, the $a$-spacing of

TABLE IV Composition of the 2:17 phase in the $Ce_{1-x}Al_xCo_5$ alloys

| Specimen composition | | Proportion of the two phases βCo–Al/2:17 in the alloy | at% Al in 2:17-phase | at% Co in 2:17-phase | at% (Co + Al) in 2:17-phase | at% Ce in 2:17-phase |
|---|---|---|---|---|---|---|
| $x$ | at% Al | | | | | |
| 0.24 | 4 | 0/100 | 4.0 | 83.3 | 87.3 | 12.7 |
| 0.36 | 6 | 1/6.96 | 6.0 | 81.8 | 87.8 | 12.2 |
| 0.42 | 7 | 1/3.02 | 7.5 | 79.6 | 87.1 | 12.9 |
| 0.48 | 8 | 1/1.93 | 7.8 | 79.0 | 86.9 | 13.1 |
| 0.54 | 9 | 1/2.00 | 9.1 | 79.4 | 88.5 | 11.5 |
| 0.60 | 10 | 1/1.40 | 10.7 | 77.9 | 88.6 | 11.4 |

TABLE V Lattice parameters of the $PrCo_5$-type phase in the $Pr_{1-x}Al_xCo_5$ alloys

| Sample $x$ | Al composition (at%) | $a$(Å ± 0.004) ($c/a$ = 0.792) |
|---|---|---|
| 0 | 0 | 5.033 |
| 0.06 | 1 | 5.033 |
| 0.12 | 2 | 5.035 |
| 0.18 | 3 | 5.034 |

TABLE VI Lattice parameters of the $Pr_2Co_{17}$-type phase in the $Pr_{1-x}Al_xCo_5$ alloys

| Sample $x$ | Al composition (at%) | $a$(Å ± 0.004) ($c/a$ = 1.446) |
|---|---|---|
| 0.06 | 1 | 8.451 |
| 0.12 | 2 | 8.456 |
| 0.18 | 3 | 8.451 |
| 0.24 | 4 | 8.457 |
| 0.30 | 5 | 8.463 |
| 0.36 | 6 | 8.467 |
| 0.48 | 8 | 8.483 |
| 0.54 | 9 | 8.486 |

the 2:17 phase is constant within the experimental error of ± 0.004 Å.

The alloy containing 4 at % Al was shown by X-ray diffraction and metallography (Fig. 4) to be one phase and of the rhombohedral structure type.

Alloys in the composition range $0.3 \leqslant x \leqslant 0.6$ (i.e. 5 to 10 at % Al) were, (as mentioned previously), extremely difficult to melt, and it was not possible to produce samples containing 7 or 10 at % Al which did not either loose material during the melt or deteriorate rapidly on exposure to air. All the alloys in this series consisted of the 2:17 phase and the fcc $\beta$Co–Al phase which was present in the equivalent Ce alloys. The samples containing 7 and 10 at % Al, which were Pr deficient, showed weak reflections from the 2:17 phase, strong reflections from the $\beta$Co–Al phase and also from the bcc AlCo phase which is of the CsCl-type structure. The lattice parameters of the 2:17 phase are plotted in Fig. 2, which does not include the results from the 7 and 10 at % Al alloys. It can be seen that, in the range 1 to 4 at % Al, the $a$-spacing stays virtually constant and then starts to increase with Al content in a way similar to that of the Ce alloys, although the slope of the line is not as steep as in the Ce case. An approximate extrapolation from the sharply increasing part of the graph to the "Zero % Al" composition gives a value slightly greater than that quoted for $Pr_2Co_{17}$ in [10] but one that is considerably greater than that quoted in [6].

Because of the melting problems referred to earlier, no attempt has been made to determine the variation of composition of the 2:17 phase with Al content of the alloy, although, since a vir-

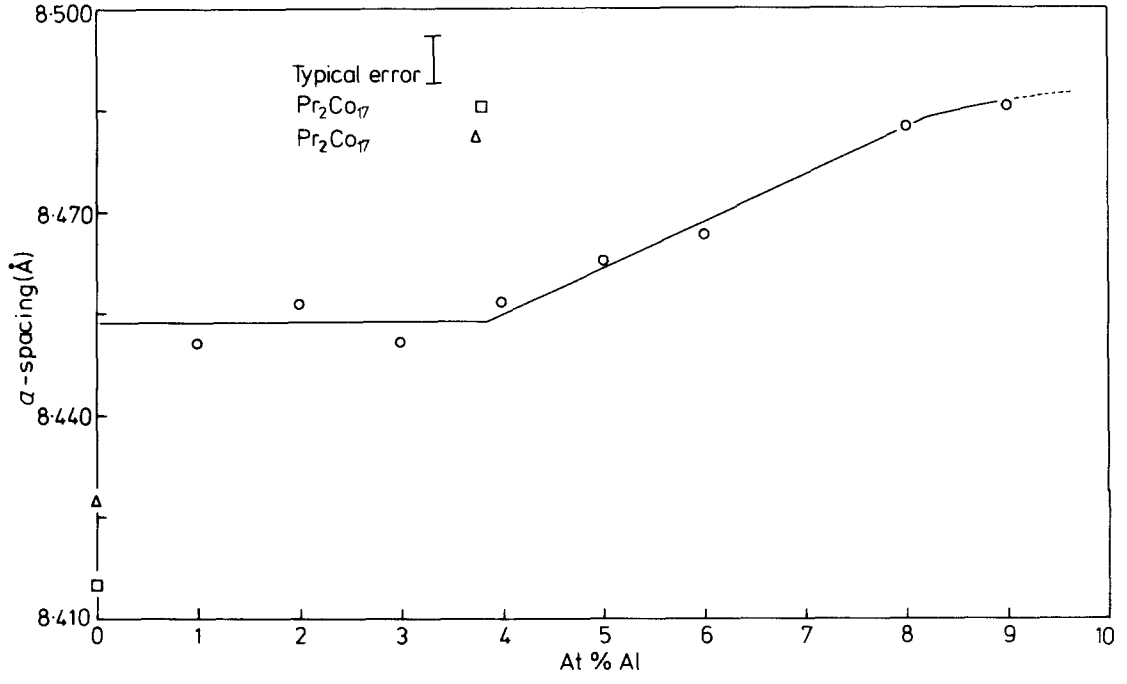


*Figure 2* Lattice spacings of the $Pr_2Co_{17}$-type phases against composition of the Pr–Co–Al alloys.

tually single-phase compound is produced at a composition of $Pr_{0.76}Al_{0.24}Co_5$, it is probable that the Pr system behaves in much the same way as the Ce system.

It has thus been shown that there is virtually no solubility of Al in either $CeCo_5$ or $PrCo_5$ when the Al is substituted for the rare-earth element, and that the Al additions stabilize the 2:17 structure. Washko *et al.* [3] have investigated the magnetic and crystallographic properties of the alloys $Sm_{0.9}Z_{0.1}Co_5$, where $Z$ represents Hf, Zr, Mg, Sb, Sn, Pb, Ca, Bi, Se and Te and these workers showed that Hf substitution stabilizes the 1:5 structure while the other substitutions favour the 2:17 structure. These results showed no apparent correlation between the magnetic and crystallographic properties of the ternary alloys and the atomic radius or crystallographic structure of the substituting element.

Analysis of the results for the Ce–Al–Co alloys in the present work shows that the 2:17 phase (for the 4 at% Al alloy) can be represented by the formula $Ce_2(Al_{0.76}Ce_{0.41}Co_{15.83})$ if it is assumed that there are no constitutional vacancies in the structure and that all the Ce-sites in the $Ce_2Co_{17}$ lattice are occupied by Ce-atoms and the Co-sites are occupied by a mixture of Co-, Al- and Ce-atoms. The fact that, for both the alloy systems studied, an approximate extrapolation from the composition range where there is a linear variation of $a$-spacing with % Al to the zero % Al composition gives a slightly higher value of $a$ than that quoted in the literature for the corresponding binary $R_2Co_{17}$ alloy ($R$ = Ce or Pr) is consistent with the hypothesis that a small proportion of the Co-sites in the $R_2Co_{17}$ lattice are occupied by the larger $R$-atoms. The progressive rise in the $a$- and $c$-spacings for the 2:17 phase in the composition range 4 to 10% Al in both the Ce- and Pr-systems can be understood in terms of the progressive substitution of Co by the larger Al-atoms. From the intensity measurements on the 2:17 phases obtained in the present work it was not possible to determine whether or not there is ordering of Al on Co-sites or substitution of $R$ on Co-sites. However, Oesterreicher [11, 12] has shown that addition of Al to $RCo_5$ and $R_2Co_{17}$ (where $R$ = Pr or Sm) to form alloys represented by $R_{0.167}Co_{0.883-x}Al_x$ and $R_{0.105}Co_{0.895-x}Al_x$ produces one-phase material for $0.2 \geqslant x \geqslant 0$ with a random distribution of Al- and Co-atoms on the original Co-sites.

## 3.2. Metallographic studies

Figs 3 and 4 show a collection of photomicrographs (of magnification × 500) of the $R_{1-x}Al_xCo_5$ alloys for $0 \leqslant x \leqslant 0.36$. Each sample is photographed in planes perpendicular to and parallel to the solidification direction of the arc-melted buttons.

### *3.2.1. $Ce_{1-x}Al_xCo_5$ alloys*

The binary $CeCo_5$ alloy is shown in Figs 3a and 3b. There is considerable variation in grain size across the specimen, but the average grain size is approximately 100 $\mu$m. There is no evidence of any second phase in this sample. However the $Ce_{0.94}Al_{0.06}Co_5$ alloy is clearly two-phase, with the 2:17 phase (light areas in Figs 3c and d) tending to concentrate around the grain boundaries but with some precipitation within the grains. Fig. 3d shows that the 2:17 phase tends to be extended along the solidification direction. The grain boundaries are not well defined in this micrograph.

In the $Ce_{0.88}Al_{0.12}Co_5$ alloy the grain boundaries are still defined to some extent by the 2:17 phase (light areas in Figs 3e and f), the original 1:5 phase persists (dark areas in Figs 3e and f) and there are also large regions which consist of an intimate mixture of the two phases. In this alloy the "mixed regions" are extended along the solidification direction.

The $Ce_{0.82}Al_{0.18}Co_5$ alloy consists chiefly of a very intimate mixture of the 1:5 and 2:17 phases, though the grain boundaries are still well defined, but now by the darker 1:5 phase which is surrounded by a "denuded" zone consisting of the 2:17 phase (Figs 3g and h). In marked contrast to this microstructure the $Ce_{0.76}Al_{0.24}Co_5$ (4 at% Al) alloy appeared to be one-phase in character (Figs 3i and j) though the X-ray results indicate that the hexagonal and rhombohedral forms of the 2:17 compound occur in approximately equal concentrations in this alloy.

All the alloys in the composition range $Ce_{0.70}Al_{0.30}Co_5$ to $Ce_{0.40}Al_{0.60}Co_5$ were in the two-phase condition, the second phase being distributed uniformly throughout the matrix, and its proportion increasing with increasing Al-content of the alloys. The samples containing 5 at% Al are shown in Figs 3k and l. The X-ray diffraction studies mentioned earlier indicate that the matrix is the 2:17 compound and the second phase is a solid solution of Al in the high temperature fcc phase of cobalt ($\beta$Co). The $\beta$Co solid solution

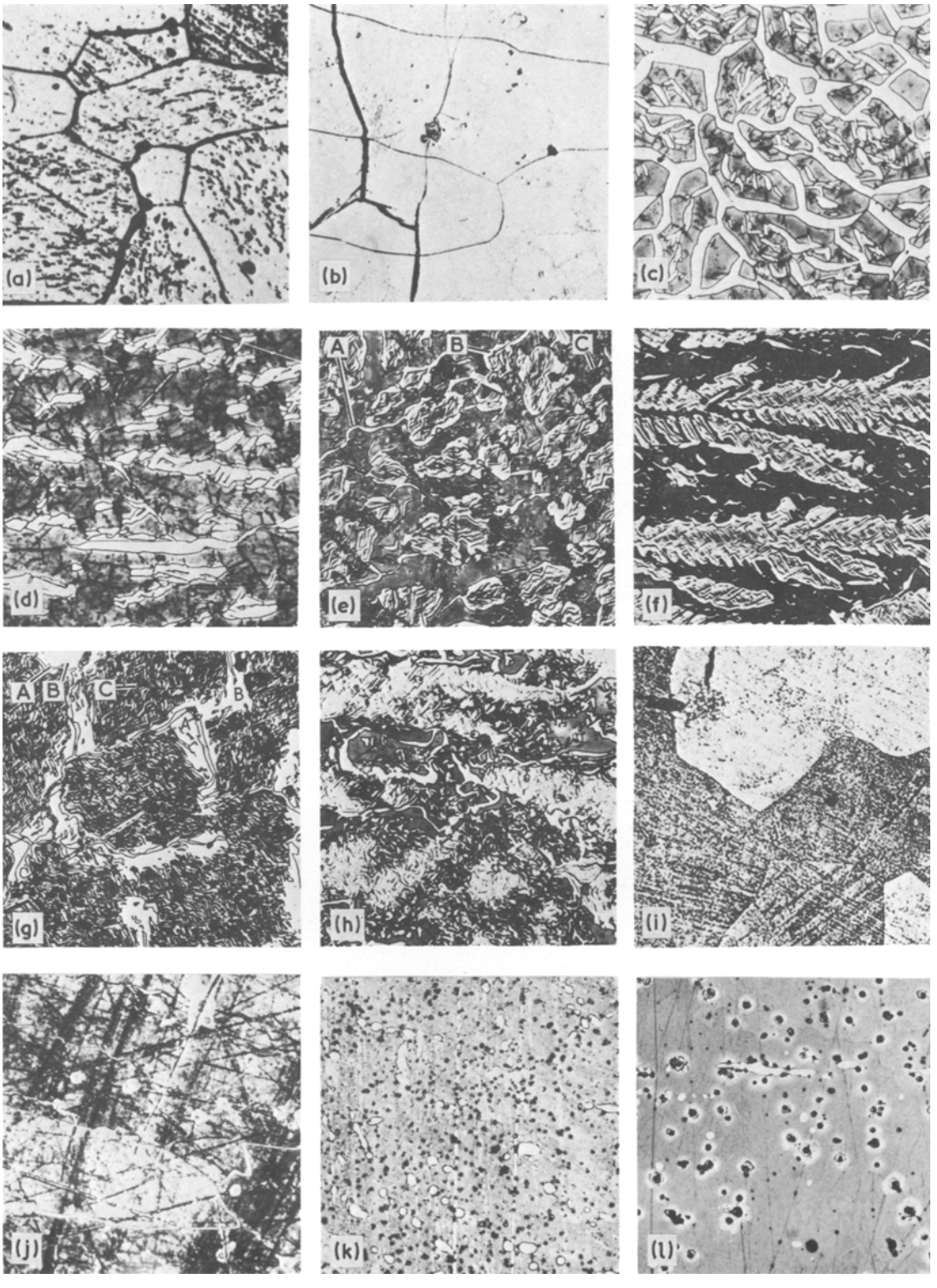


*Figure 3* (a, b) Micrographs of $CeCo_5$ (× 500); (c, d) micrographs of $Ce_{0.94}Al_{0.06}Co_5$ (× 500); (e, f) micrographs of $Ce_{0.88}Al_{0.12}Co_5$ (× 500); (g, h) micrographs of $Ce_{0.82}Al_{0.18}Co_5$ (× 500); (i, j) micrographs of $Ce_{0.76}Al_{0.24}Co_5$ (× 500); (k, l) micrographs of $Ce_{0.70}Al_{0.30}Co_5$ (× 500).

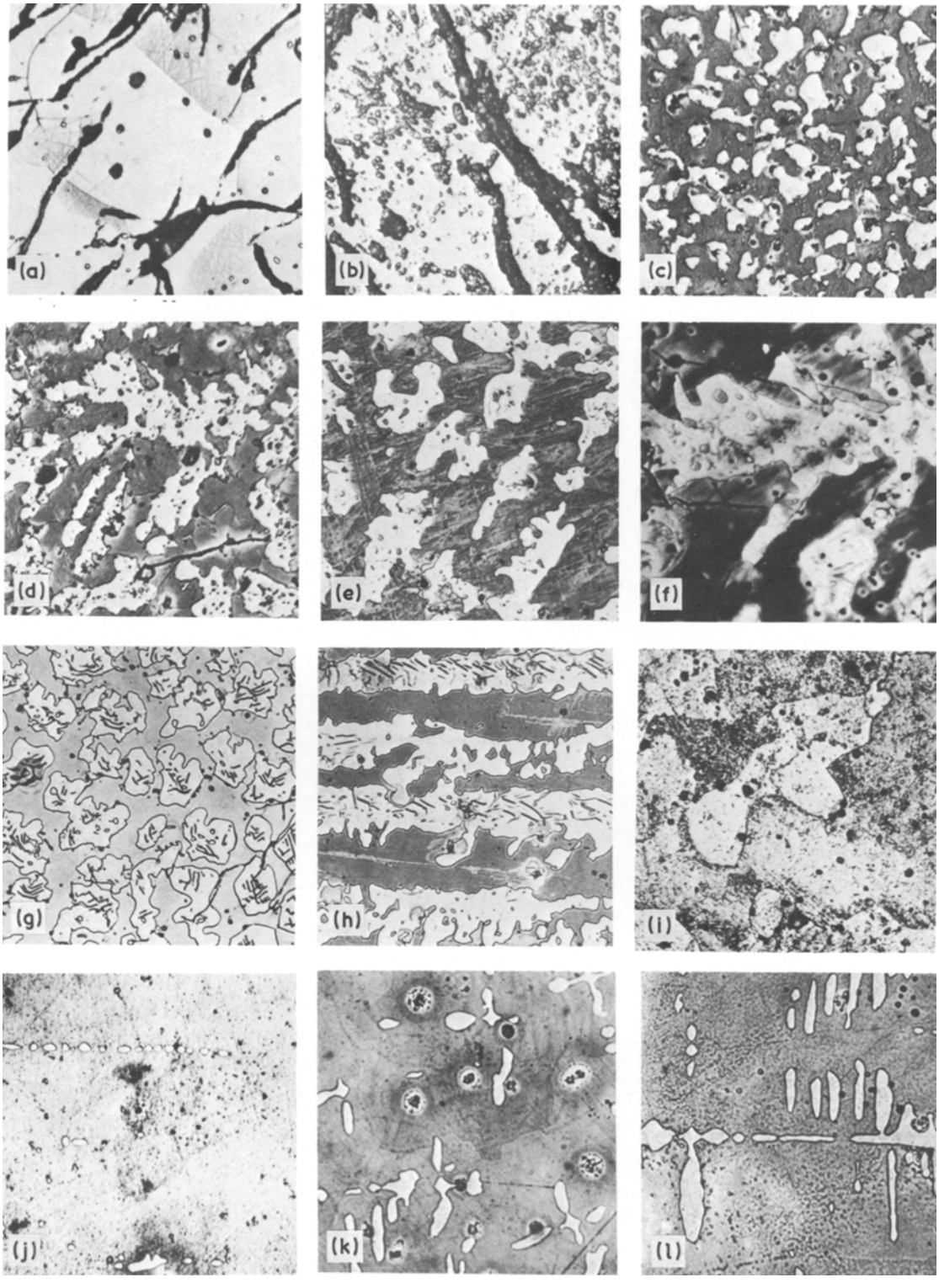


*Figure 4* (a, b) Micrographs of $PrCo_5$ (× 500); (c, d) micrographs of $Pr_{0.94}Al_{0.06}Co_5$ (× 500); (e, f) micrographs of $Pr_{0.88}Al_{0.12}Co_5$ (× 500); (g, h) micrographs of $Pr_{0.82}Al_{0.18}Co_5$ (× 500); (i, j) micrographs of $Pr_{0.76}Al_{0.24}Co_5$ (× 500); (k, l) micrographs of $Pr_{0.70}Al_{0.30}Co_5$ (× 500).

phase forms precipitates which exhibit a 4-fold symmetry when viewed in a direction perpendicular to the solidification direction of the specimen (Fig. 3k), there is also alignment of the second phase along the solidification direction (Fig. 3l).

As observed in the previous section, the addition of Al stabilizes the 2:17 phase with respect to the 1:5 phase and this indicates a large homogeneity region for the $Ce_2(Al + Co + Ce)_{17}$ phase extending to the Ce-rich region of the ternary phase field. The 1:5 phase (by analogy with $SmCo_5$ [13]) probably extends to the Co-rich side of the 1:5 stoichiometry and therefore the alloy containing 1 at% Al probably exists in the 1:5 phase field at high temperature, and, on cooling, passes into a two-phase region consisting of the 1:5 and 2:17 phases with the 2:17 phase (light areas in Figs 3c and d) deposited at the grain boundaris and, by a Widmanstätten-type precipitation, within the grains.

The microstructure of the 2 at% Al alloy is also consistent with this composition being within the 1:5 phase field at high temeprature. On cooling, 2:17 phase material is deposited at the grain boundaries (region A, Fig. 3e) and as a fine Widmanstätten precipitate within the grains. Because of the higher proportion of 2:17 phase in this alloy the Widmanstätten precipitation is far more extensive than in the previous case. The islands of Widmanstätten are bounded by areas of the 2:17 phase (region B in Fig. 3e) and are themselves in a matrix of grey coloured 1:5 phase (region C in Fig. 3e). The 2:17 phase of region B, and at the grain boundaries, is probably derived from the Widmanstätten region by segregation during the homogenization process.

The microstructure of the alloy containing 3 at% Al is consistent with this alloy existing in the 2:17 phase field at high temperatures rather than the 1:5 phase field as in the previous alloy. Thus on cooling it passes into a 2:17/1:5 two-phase region and it is now the 1:5 phase which is deposited at the grain boundaries (area A, Fig. 3g) and as a Widmanstätten precipitate in the 2:17, within the grains (area C Fig. 3g). The light areas of 2:17 phase (region B, Fig. 3g) surrounding the 1:5 grain boundary precipitates are due to the diffusion of the 1:5 phase from the Widmanstätten precipitate to the grain boundary, thus producing a 1:5 denuded zone.

### 3.2.2. $Pr_{1-x}Al_xCo_5$ alloys

The binary alloy is shown in Figs 4a and b. A variety of etches failed to define the grain boundaries but there was no evidence of any second phase in this alloy.

The alloys $Pr_{0.94}Al_{0.06}Co_5$, $Pr_{0.88}Al_{0.12}Co_5$ and $Pr_{0.82}Al_{0.18}Co_5$, are all in the two-phase condition, though unlike the corresponding Ce–Co–Al alloys, the 2:17 phase appears to be formed by a peritectic reaction and is distributed uniformly throughout the 1:5 matrix. These microstructures are more characteristic of liquid → solid reactions rather than the solid-state precipitation processes observed in the corresponding Ce-alloys. The 2:17 phase appears as light areas in Figs 4c to h and there is evidence of a Widmanstätten precipitate within the 2:17 in the $Pr_{0.82}Al_{0.18}Co_5$ alloy (Figs 4g and h).

The $Pr_{0.76}Al_{0.24}Co_5$ alloy is shown in Figs 4i and j; some second phase material was present, but this was a very small proportion of the whole sample.

Micrographs of the Pr–Co–Al alloys containing 5 at% Al are shown in Figs 4k and l and are very similar to those obtained from the corresponding Ce–Co–Al alloys.

### 3.2.3. Magnetic measurements

The magnetic balance used for the Curie-point determination of the alloys in this work is most often used to study the behaviour of diamagnetic and paramagnetic specimens, either as pure materials, or containing very small amounts of ferromagnetic impurities. For measurements on paramagnets and diamagnets, correction for field dependence caused by the presence of ferromagnetic impurities is made by measuring susceptibility, $\chi$, at different fields, $H$, and extrapolating to infinite field a plot of susceptibility against $H^{-1}$. This is the method of Honda [14] and Owen [15] in which the apparent susceptibility, $\chi_H$, at field $H$, is related to the true susceptibility $\chi_\infty$ in an extremely high field by the equation

$$\chi_\infty = \chi_H - \frac{c\sigma_s}{H}, \qquad (1)$$

where $\sigma_s$ is the saturation specific magnetization of the impurity which is present in a concentration by weight of $c$.

A ferromagnet, below its Curie temperature, does not have a constant susceptibility as most ferromagnets are saturated at low fields, and hence $\chi$ $(M/H)$ varies with field, where $M$ is the magnetization $(M = (B/\mu_0) - H$ where $B$ is the magnetic

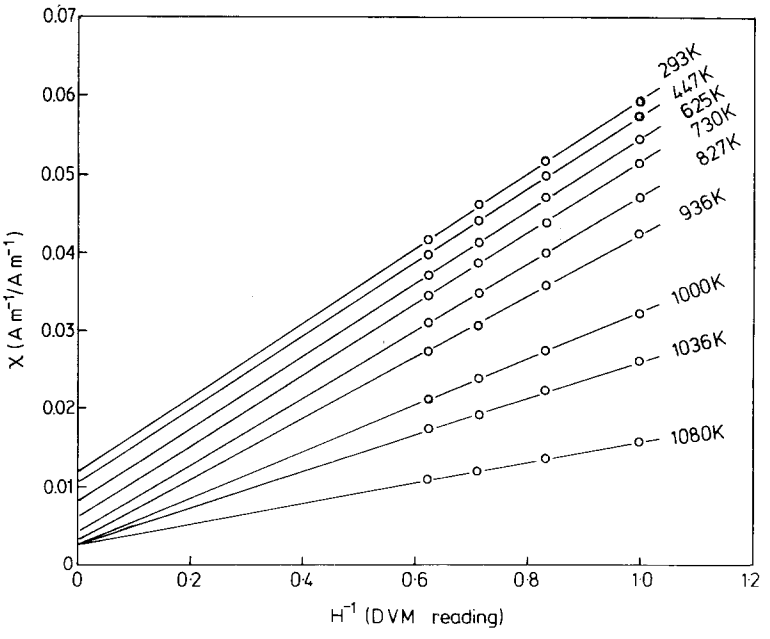


*Figure 5* Honda and Owen plot at various temperatures for $Pr_{0.76}Al_{0.24}Co_5$.

flux density in Tesla). In contrast, the field needed to saturate a typical paramagnet at room temperature is of the order of $10^8$ to $10^9$ $Am^{-1}$, and therefore under "normal" conditions $\chi$ is constant.

The ferromagnetic $R_{1-x}Al_xCo_5$ ($0 \leqslant x \leqslant 0.24$) alloys investigated in this work are not saturated until a field of $> 4 \times 10^5$ $Am^{-1}$ is applied. Therefore, in the above expression where $c = 1$, the magnetization (given by the gradient of the $\chi$ versus $H^{-1}$ plot) is not the saturation magnetization, but the magnetization at the highest field attainable in the magnetic balance. If the material is saturated $\chi_\infty$ should be zero, but again this is not the case in this work. For the present purposes this does not matter since the absolute values of the magnetizations are not required and the technique is used only to determine the Curie temperature of the alloys as an aid to thermomagnetic phase analysis. As expected, the plots of the $\chi$ versus $H^{-1}$ graphs at different temperatures showed marked changes in gradient around the Curie points of the phases present in the alloys. As a typical example, the Honda and Owen plot for $Pr_{0.76}Al_{0.24}Co_5$ at various temperatures is shown in Fig. 5. The magnetization against temperature curves derived from such plots (Figs 6 and 7) are used to determine the Curie temperatures of the phases present. The good agreement with the published Curie temperatures for the $RCo_5$ phases indicates the reliability of this method of determining Curie temperatures.

The graph of the "Honda and Owen gradient" or "unsaturated magnetization", $M$ against temperature for $CeCo_5$ is shown in Fig. 6a. The appearance of this curve is very like that of a typical ferromagnet up to a temperature of about 745 K, but beyond this point there is a flattening of the curve up to a temperature of about 943 K where there is a further drop in magnetization to a level which then appears to remain constant. The first sharp drop in the magnetization curve extrapolates to a value corresponding to the Curie point of $CeCo_5$ (~ 730 K). The plateau region probably corresponds to the presence of $Ce_2Co_{17}$, formed as a result of either slight oxidation of the $CeCo_5$ or its eutectoid decomposition into $Ce_2Co_7 + Ce_2Co_{17}$ [16]. The residual magnetization beyond this point is probably due to the presence of free cobalt.

The magnetization against temperature curve for the $Ce_{0.88}Al_{0.12}Co_5$ alloy (2 at % Al) (Fig. 6b) shows only a slight dip at 726 K, the magnetization then rising slightly before decreasing sharply towards the Curie temperature of the 2:17 phase. There is then a further slight increase in magnetization, which after 1122 K rapidly decreases. The dip in the magnetization curve at 726 K is an indication of the presence of the $CeCo_5$ phase (Curie temperature 730 K) and the slight increase beyond this point is probably due to the transformation of some of the $CeCo_5$ to $Ce_2Co_{17}$. The further decrease in magnetization extrapolates to the $T_c$

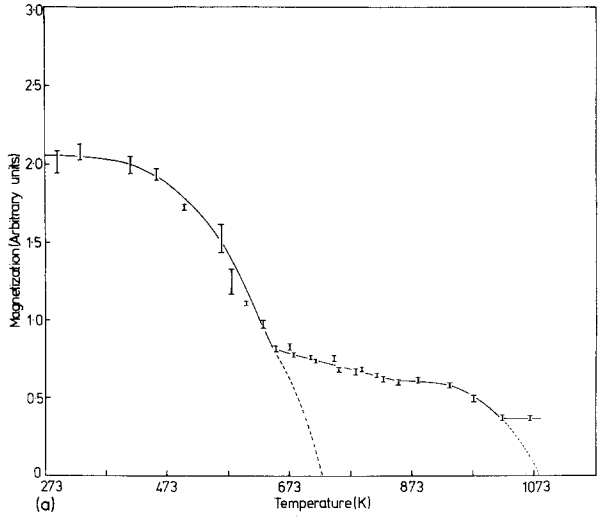


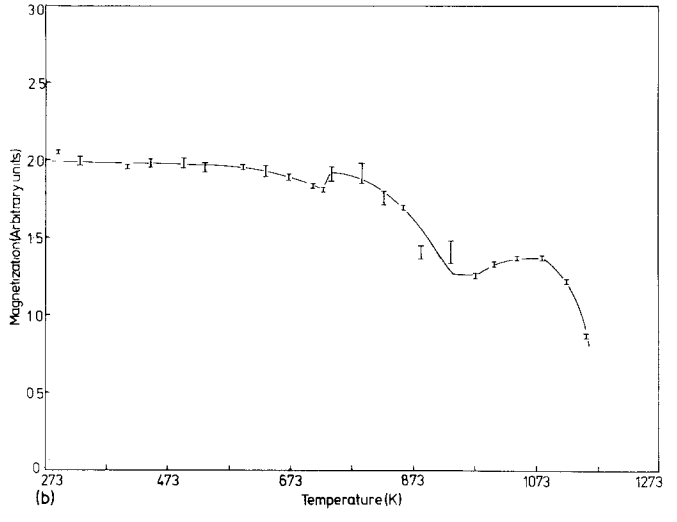


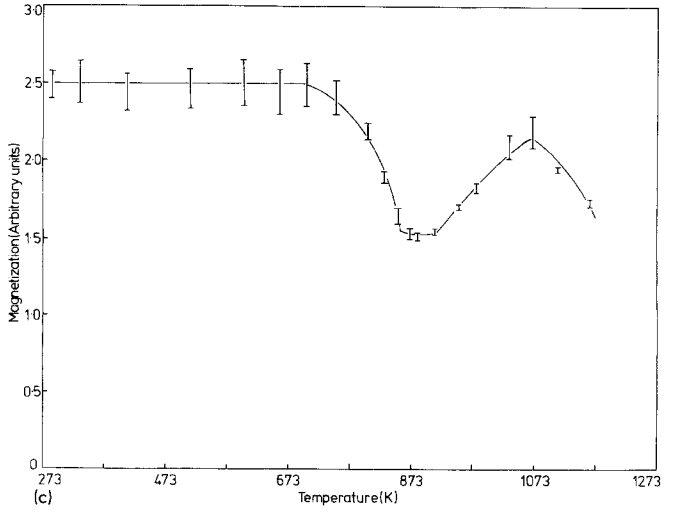


*Figure 6* (a) Magnetization against temperature curve for $CeCo_5$, (b) magnetization against temperature curve for $Ce_{0.88}Al_{0.12}Co_5$; (c) magnetization against temperature curve for $Ce_{0.76}Al_{0.24}Co_5$.

of the $Ce_2(Co + Al + Ce)_{17}$ phase. The last part of the curve may again be explained by the formation of free cobalt.

The magnetization against temperature graph (Fig. 6c) for the one-phase 2:17 alloy (4 at % Al) is a smooth curve which extrapolates to a Curie temperature of ~ 1030 K (compared to a $T_c$ of 1083 K for $Ce_2Co_{17}$). At temperatures above about 1020 K the magnetization starts to increase, again due to the formation of free cobalt. Because of the formation of a second magnetic phase it is difficult to determine precisely the Curie point of the $Ce_2$ $(Co + Ce + Al)_{17}$ phase, but the value quoted above is thought to have an accuracy of around ± 10 K.

The magnetization against temperature curve for the binary $PrCo_5$ alloy (Fig. 7a) remains constant with temperature up to approximately 575 K and then dips sharply at about 900 K. Beyond this point the magnetization increases with temperature up to about 1070 K before starting to decrease one more. The first sharp dip in the curve extrapolates to a temperature of around 980 K, which compares well with the value of $T_c$ of 912 K (for $PrCo_5$) quoted in [17]. There seems to be no evidence for the formation of $Pr_2Co_{17}$ from this alloy, but free cobalt does seem to be formed, as in the case of the Ce-alloys.

The magnetization against temperature curve of the $Pr_{0.88}Al_{0.12}Co_5$ alloy is shown in Fig. 7b. The graph shows two distinct steps, the first of which indicates the presence of $PrCo_5$ and the second, that of the $Pr_2$ $(Co + Pr + Al)_{17}$ phase. The magnetization remaining beyond about 1100 K is assumed to be due to the presence of free cobalt.

The magnetization against temperature graph for the one-phase 2:17 alloy containing 4 at % Al (Fig. 7c) is a smooth curve which extrapolates to a Curie temperature of about 1100 K (compared with 1171 K for $Pr_2Co_{17}$). At temperatures above about 1070 K the magnetization starts to increase, again due to the formation of free cobalt.

Substitution of Al for $R$ in $RCo_5$ to form the $R_2(Co + Al + R)_{17}$ alloys causes a structural change without increasing the number of Co-atoms per formula unit, though the Curie temperatures of the ternary 2:17 phases in both systems are much closer to those of the corresponding $R_2Co_{17}$ phases than to those of the $RCo_5$ phases. This indicates that, for the $R_{1-x}Al_xCo_5$ alloys, the Curie temperatures of the phases produced are strongly structure dependent.

The information supplied by the thermomagnetic phase analysis is consistent with that derived from the X-ray diffraction and metallographic results and provides the additional information of the Curie points of the constituent phases. However, it was not possible using this technique to determine either the absolute values of the magnetizations of the phases, or their relative proportions. This is because the fields used in this work were not high enough to give saturation magnetizations and the samples used were so small (typically 0.1 mg) that they were not necessarily representative of the bulk material examined in the metallographic studies.

## 4. Conclusions

(1) Substitution of Al for both Ce and Pr according to the formula $R_{1-x}Al_xCo_5$ stabilizes the 2:17 structure, one-phase alloys of the 2:17 structure type being produced for samples containing 4 at % Al. The 2:17 phases are thought to have the formula $R_2(Al_{0.76}R_{0.41}Co_{15.83})$, all the $R$-sites in the $R_2Co_{17}$ lattice being occupied by $R$-atoms and the Co-sites occupied by a mixture of Co-, Al- and $R$-atoms.

(2) Metallographic examination shows that in the case of the Ce-alloys there is an intimate mixture of the 1:5 and 2:17 phases in the range 1 to 3 at % Al whereas for the corresponding Pr-alloys the 2:17 phase seems to be produced by a peritectic reaction and exists as "islands" in the 1:5 matrix. It should be noted that only one annealing temperature was used to produce these alloys and the effects of different heat treatments on their microstructures would be of considerable interest.

(3) The magnetic measurements show that the ternary 2:17 Ce and Pr phases have Curie temperatures that are 50 K and 70 K lower than $Ce_2Co_{17}$ and $Pr_2Co_{17}$, respectively.

It is known that the presence of $Sm_2Co_{17}$ in $SmCo_5$ magnets greatly reduces their coercivity because the 2:17 phase provides sites for the nucleation of reverse domains. The coercivities of the ternary 2:17 alloys have not yet been determined and cannot therefore be compared to the binary alloys. It is also not known whether the $R_{1-x}Al_xCo_5$, 2:17 phases have their easy axis of magnetization in the basal plane or along the crystallographic $c$-direction. However Strnat and Ray [18] have shown that the addition of small

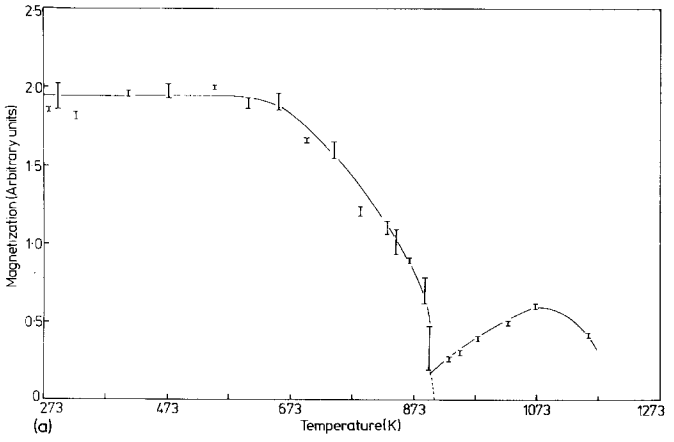


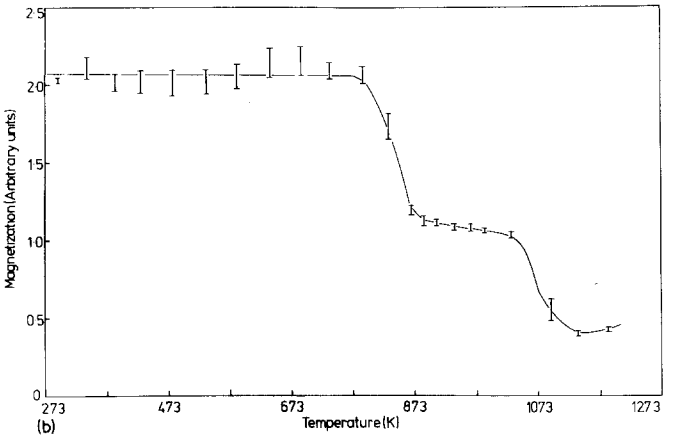


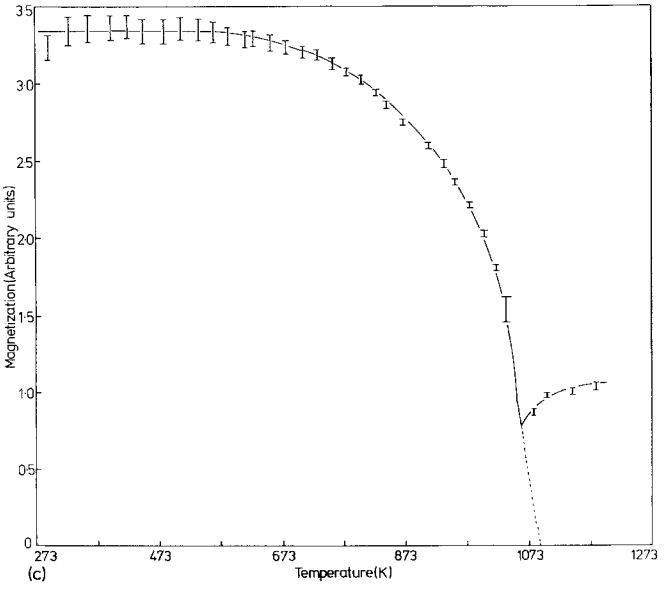


*Figure 7* (a) Magnetization against temperature curve for $PrCo_5$; (b) magnetization against temperature curve for $Pr_{0.88}Al_{0.12}Co_5$; (c) magnetization against temperature curve for $Pr_{0.76}Al_{0.24}Co_5$.

quantities of iron to $Ce_2Co_{17}$ and $Pr_2Co_{17}$ changes the undesirable easy-basal-plane anisotropy into the more desirable situation where the crystallographic $c$-axis is the only easy direction of magnetization and consequently it is important that a similar study of the ternary $R$–Co–Al alloys should be undertaken. Thus, further magnetic assessment of the ternary 2:17 phases is desirable to determine their intrinsic coercivities and anisotropy fields.


## Acknowledgements

Thanks are due to the SRC for support of the general research programme of which this work forms a part.


## References


1. J. J. BECKER, *J. Appl. Phys.* **41** (1970) 1055.
2. K. J. STRNAT, American Institute of Physics Conference Proceedings on Magnetism and Magnetic Materials No. 5, Edited by C. D. Graham, Jr and J. J. Rhyne (American Institute of Physics, New York, 1972) Part 2, p. 1047.
3. S. WASHKO, J. GERBOC and J. OREHOTSKY, *I.E.E.E. Trans. Mag.* **MAG-12** (1976) 974.
4. Goldschmidt report 4/75 Number 35 (Dec. 1975).
5. Goldschmidt report 2/79 Number 48 (May 1979).
6. W. OSTERTAG and K. J. STRNAT, *Acta Cryst.* **21** (1966) 560.
7. H. L. LUO and P. DEWEZ, *Canadian J. Phys.* **41** (1963) 758.
8. A. E. RAY, A. T. BIERMANN, R. S. HARMER and J. E. DAVIDSON, *Cobalt* **4** (1973) 103.
9. J. EVANS, Ph.D. Thesis, University of Birmingham, 1978.
10. K. H. J. BUSCHOW, *J. Less Common Met.* **11** (1966) 204.
11. H. OESTERREICHER, *ibid.* **32** (1973) 385.
12. *Idem, ibid.* **33** (1973) 25.
13. K. H. J. BUSCHOW and F. J. A. DEN BROEDER, *ibid.* **33** (1973) 191.
14. K. HONDA, *Ann. Phys. Leipzig* **32** (1910) 1048.
15. M. OWEN, *Ann. Phys. Leipzig* **37** (1912) 657.
16. K. H. J. BUSCHOW, *J. Less Common Met.* **29** (1972) 283.
17. K. J. STRNAT, *Cobalt* **36** (1967) 133.
18. K. J. STRNAT and A. E. RAY, Goldschmidt report 4/75 Number 35 (Dec. 1975) pp. 47–53.



*Received 14 April*
*and accepted 12 May 1980*